Thermochimica Acta, 61 (1983) 53–71
Elsevier Scientific Publishing Company, Amsterdam – Printed in The Netherlands

ON THE SOLID STATE PRODUCTS OF THE THERMAL DECOMPOSITION OF CONFINED AND UNCONFINED TRIAMINOTRINITROBENZENE *

EDWARD CATALANO and CLAUDIA E. ROLON
Lawrence Livermore National Laboratory, Livermore, CA 94550 (U.S.A.)
(Received 23 June 1982)

ABSTRACT

The solid state products formed by the thermal decomposition of triaminotrinitrobenzene (TATB) were examined using infrared spectroscopy and optical and scanning-electron microscopy (SEM). Several phases were observed in condensates and residues from unconfined decompositions. The residues from confined decompositions show that very little decomposition occurs until times near the time to explosion. A model for the unconfined decomposition is presented.

INTRODUCTION

The unusual stability of triaminotrinitrobenzene (TATB) arises because of the presence of a large number of intra- and intermolecular hydrogen bonds [1]. A measure of this stability is reflected in the thermal decomposition kinetics. The decomposition of unconfined TATB has been the subject of several investigations [2–5]. Integral thermal decomposition kinetics of confined TATB using the one-dimensional time-to-explosion (ODTX) technique have been reported [6] as have Henkin tests [7]. We have also reported on the gaseous products and the kinetics of their evolution from the thermal decomposition of confined TATB [8] and the enthalpic changes during decomposition of unconfined TATB [9].

This work is a preliminary study of the solid state products obtained as part of these previous studies. Solid state products were examined by infrared spectroscopy, optical microscopy, and scanning electron microscopy (SEM) to establish the number of phases present after an isothermal treatment. Even though no information was obtained that identifies these products, a generalized model of the decomposition of unconfined TATB is presented on the basis of the observations made.

* Work performed under the auspices of the U.S. Department of Energy by the Lawrence Livermore National Laboratory under contract number W-7405-ENG-48.

0040-6031/83/0000–0000/$03.00

EXPERIMENTAL

Experimental details have been reported for confined [8] and unconfined thermal decompositions [9] of the TATB whose analysis is shown in Table 1 of ref. [9]. In addition, an ODTX run at 597 K was repeated (the experimental details are in ref. [6]). After explosion ($t = 2.69$ min), numerous dendritic crystals were found just outside the cavity. The TATB used in the latter ODTX test was LLNL label B-266. A similar vapor-phase grown crystalline

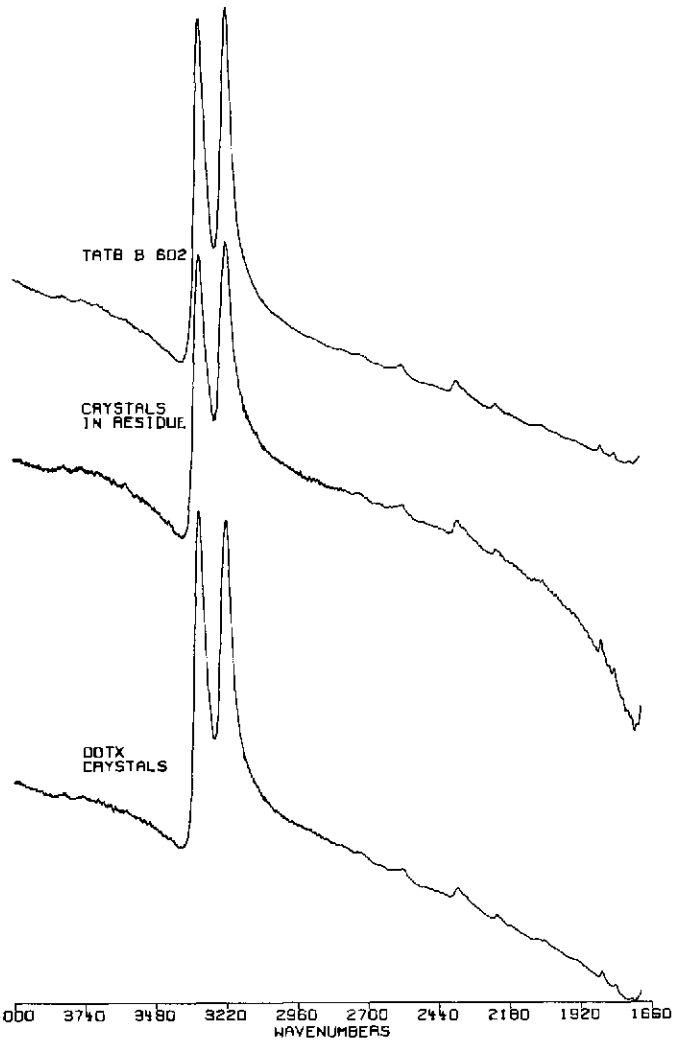

Fig. 1. The infrared spectra of the "crystalline" phase found in residues of a confined TATB decomposition and of the crystalline products from the ODTX experiment as compared with that of the starting TATB material.

product had been found in the original work [6] from runs at 597 K. X-Ray powder patterns were taken of the product crystals from the original ODTX runs. However, ODTX runs at other temperatures did not yield as well-defined crystalline products.

There were fives types of product: (a) the residues obtained from the confined isothermal runs [8]; (b) a well-crystallized material that was part of the residues from confined samples held at temperature for times in the range of 0.75–0.85 of the time to explosion, t_x [8], (this crystalline material was separated from the bulk of the residue for spectral examination); (c) condensates deposited after explosion from the ODTX run at 597 K; (d) the

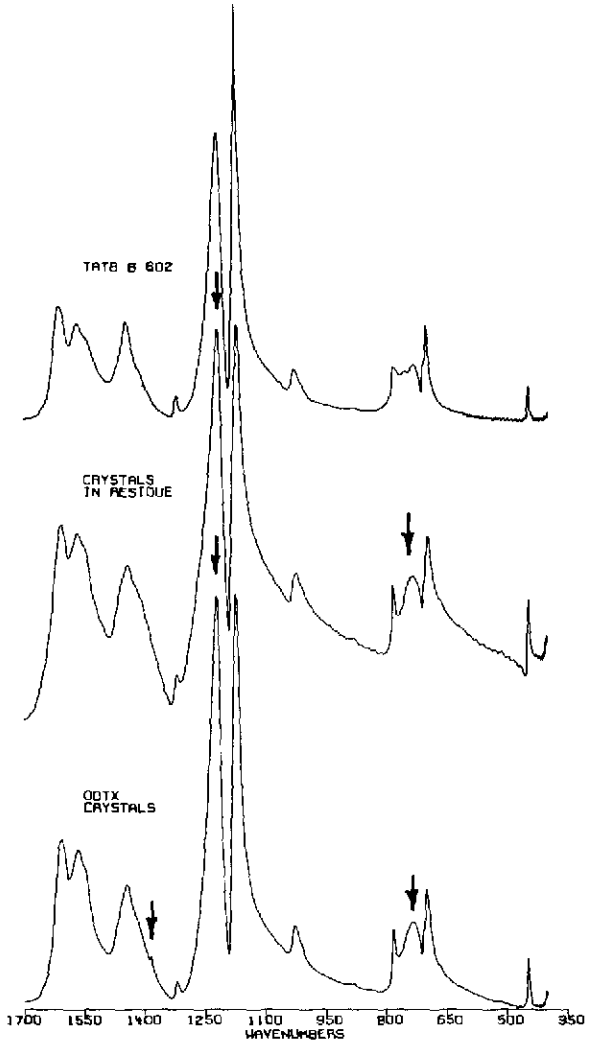

Fig. 2. The infrared spectra of the "crystalline" phase found in the residues of a confined TATB decomposition and of the crystalline products from the ODTX experiment as compared to the starting TATB material. Arrows point to the minor spectral changes.

condensates obtained from the unconfined isothermal runs [9]; and (e) the residues obtained from unconfined isothermal runs.

RESULTS

Spectral studies

Infrared spectra of TATB and an assignment of band frequencies to vibrational modes have been reported by Deopura and Gupta [10] and by Towns [11]. Our TATB spectra appear to be in complete agreement with

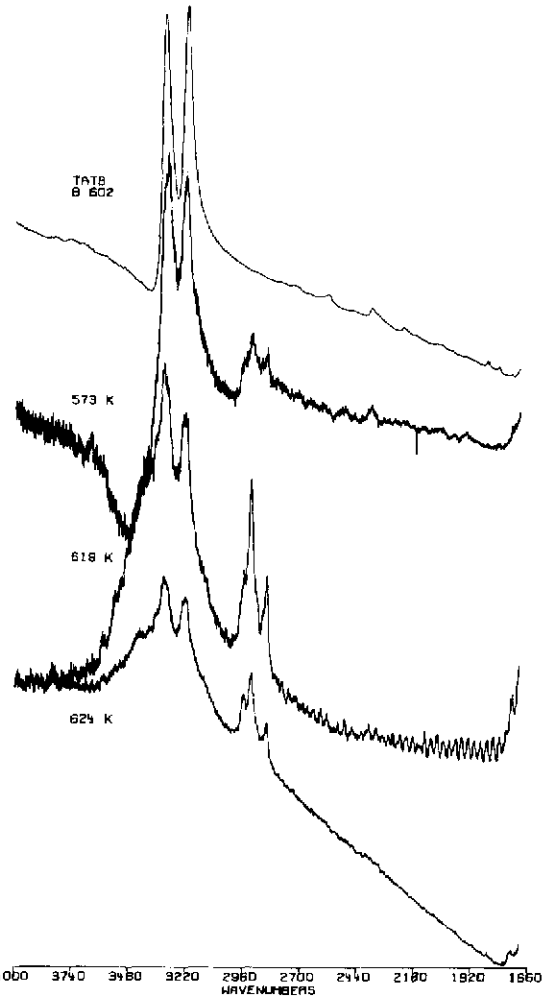

Fig. 3. The spectra of three condensates generated in unconfined TATB decompositions as compared with the starting TATB material.

both references. We prefer Towns' band assignments [11] however, as they appear to be more self-consistent.

Solid state products from confined TATB decomposition [6,8]

Figures 1 and 2 are typical spectra of the original TATB, the crystalline material found within the residues, and the condensate from the ODTX run ($T = 597$ K, $t = 2.69$ min). The spectral features of these two solid state products are very similar to those of TATB. Differences are: (1) an increase in intensity of the band at 1222 cm^{-1} relative to that at 1179 cm^{-1}; (2) the coalescence of the TATB doublet at 749 and 729 cm^{-1} into a single band for both products; and (3) the appearance of a band at 1381 cm^{-1}. The

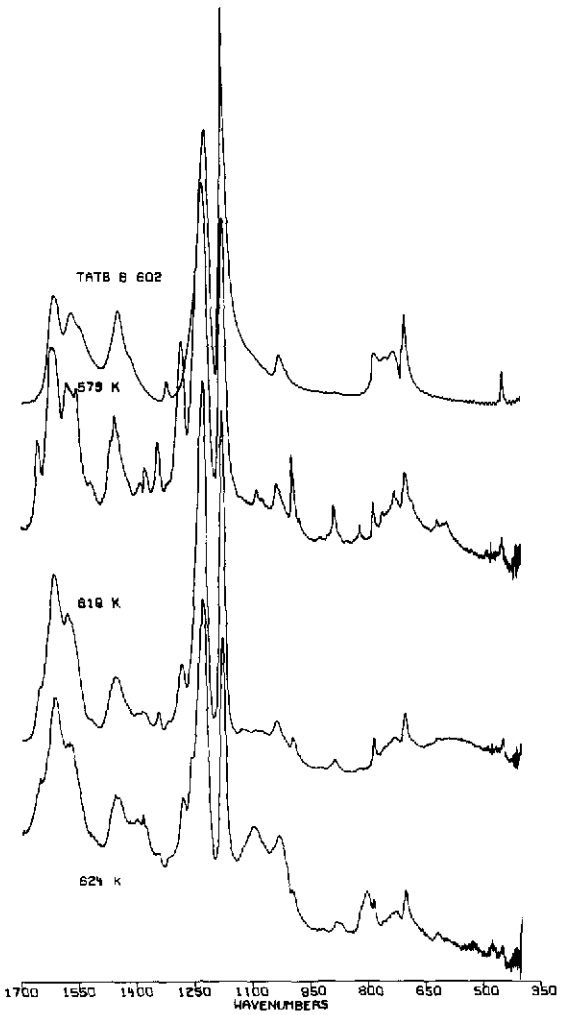

Fig. 4. The spectra of three condensates generated in unconfined TATB decompositions as compared with the starting TATB material.

TABLE I

TATB and condensate spectral features with assignment for vibrational modes of TATB

TATB	Condensate spectra (wavenumbers)			Assignment [12]
	573 K	619 K	624 K	
3820 vvw				
3750 vvw				
3690 vvw	3700 vw			
	3615 w			
3590 vvw	3590 w	3590 w		
		3420 m	3430 m	
		3379 m	3383 m	
	3410 w			
			3356 w	
3316 vs	3316 vs	3320 vs	3325 s	NH_2 (ν_a)
	3302 vs	3302 vs		
		3239 vs	3226 s	
3217 vs	3217 vs	3217 vs		NH_2 (ν_s)
	3145 vw			
	3063 vw			
	2960 m	2956 ms	2960 s	
	2928 m	2924 vs	2924 vs	
	2852 m	2852 s	2852 s	
	2785 vw			
2726 vvw	2700 vw			
2654 vvw				
	2645 vw			
	2590 vw			
2573 vw				NO_2 (ν_a)+ϕ_4
	2500 w			
	2375 w			
2365 vw				NH_2 (δ)+NO_2 (γ)
2227 vw				NO_2 (δ)+ϕ_2
2168 vvw				
2060 vvw				
1845 vw				2 NH_2 (τ)+ϕ_3
1795				NH_2 (ν_s)−ϕ_3
	1657 s	1657 m	1657 w	
1616 s	1616 s	1616 s	1611 s	NH_2 (δ)
	1583 s	1583 m		
		1573 m	1575 m	
1568 s				ϕ_1
	1558 s			
1548 m				NO_2 (ν_a)
	1519 m	1519 w		
		1507 vw		
	1463 s			
	1456 s	1456 s		
1446 s	1446 s	1446 s	1446 s	ϕ_2

TABLE 1 (continued)

TATB	Condensate spectra (wavenumbers)			Assignment [12]
	573 K	619 K	624 K	
1415 w				ϕ_3
	1390 m	1385 s	1385 m	
	1377 s			
	1344 s	1344 m		
1321 m	1321 w	1316 w	1316 w	NO_2 (ν_s)
	1283 vs	1283 s	1283 s	
			1260 s	
1222 vs	1227 vs	1227 vs	1227 vs	NH_2 ($\nu_{c\text{-}n}$)
1179 vs	1179 vs	1179 vs	1179 vs	NH_2 ($\nu'_{c\text{-}n}$)
	1128 vw	1120 vvw		
	1090 m	1084 vvw	1095 s	
	1074 w			
1064 vvw				
1029 m	1036 m	1034 m	1031 m	ϕ_4
	995 s	995 w	995 w	
	978 vw			
	922 vw			
	904 w			
881 vvw	889 s	884 m	878 m	
	868 w			
	853 w			
	820 m			
			802 s	
782 m	784 m	784 m	784 m	NO_2 (δ)
	761 w	761 w		
749 m				NO_2 (γ)
729 m	731 m	728 m	726 m	NH_2 (γ)
708 w				NO_2 (α)
700 s	700 s	703 s	700 s	NH_2 (α)
	683 w			
	619 w	619 w	619 w	
	594 w			
			525 w	
	487 w			
		471 w	479 w	
448 s	448 m	449 m	451 m	$2\times NH_2$ (τ)
			420 m	

ν = bond stretching, α = in plane deformation, τ = torsion, ϕ = phenyl, s = symmetric, δ = symmetric angle deformation, γ = out-of-plane deformation, a = anti-symmetric.

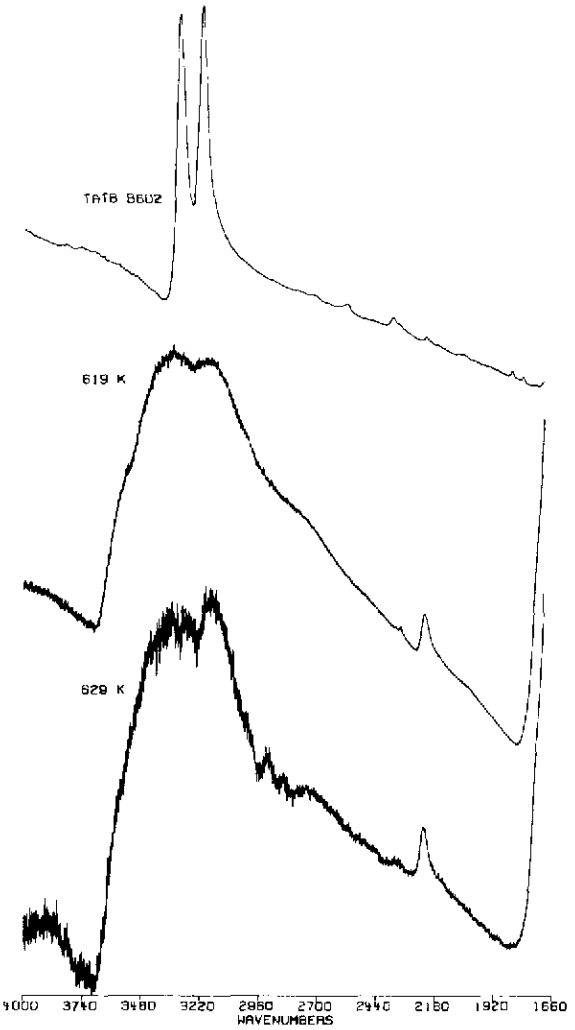

Fig. 5. The spectra of two residues generated in unconfined TATB decompositions as compared with the starting TATB material.

crystalline material found within the residues and the crystals from the ODTX experiment are almost identical and both are very similar to TATB. Arrows in Fig. 2 illustrate where differences occur in the spectra.

A sample that was held at 529 K for 78 min [8] and for which the confinement pressure was released before the TATB residue had cooled to room temperature, released a gaseous product that subsequently condensed on the walls of the gas collection apparatus. Samples of the condensate were examined spectroscopically. The spectral features were identical to those of TATB.

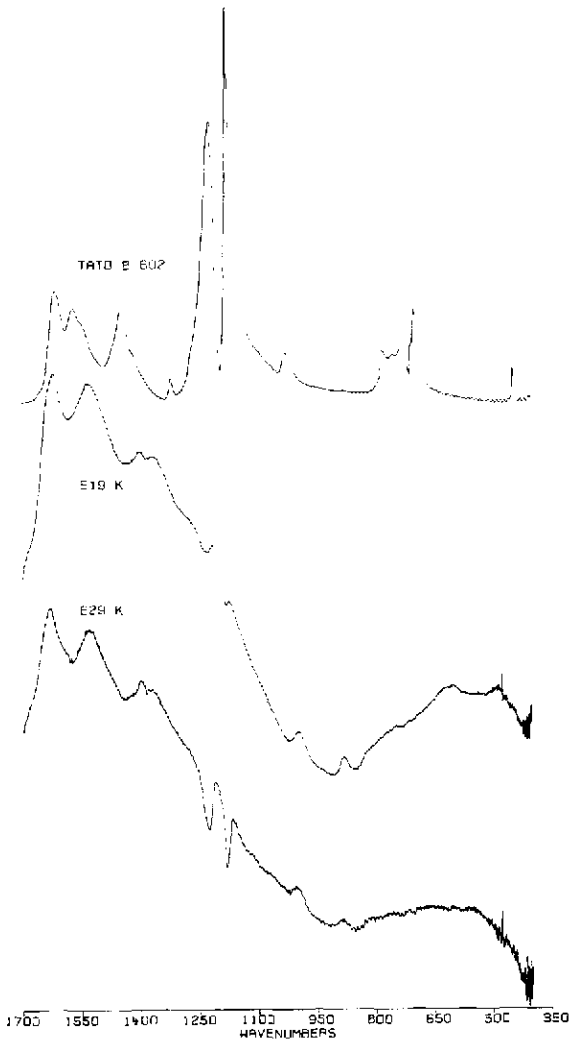

Fig. 6. The spectra of two residues generated in unconfined TATB decompositions as compared with the starting TATB material.

Solid state products from unconfined TATB decomposition [9]

There were two types of products from unconfined TATB decomposition, namely, condensates and residues. Figures 3 and 4 show the spectra of typical condensates along with the reference spectrum of TATB. Figures 5 and 6 show the spectra of typical residues along with the spectrum of TATB. It is clear from these figures that the spectra of both condensates and residues are different from TATB and also from each other. Table 1 is a listing of TATB and condensate spectral features along with the Towns' assignment for vibrational modes of TATB [11]. Table 2 is a listing of the spectral features of residues collected from decompositions at 619 K and 629 K.

TABLE 2

Unconfined residues spectra (wavenumbers)

619 K	629 K
3545 s	3880 s
3329 vs	3365 vs
3185 vs	3280 vs
2790 s	3170 vs
2334 w	3015 w
2231 m	2915 m
2040 w	2843 m
1684 w	2762 w
1619 vs	2350 w
1530 vs	2235 m
1397 w	1630 vs
1365 w	1527 vs
1275 w	1395 w
1214 w	1375 w
1174 w	1260 vw
998 m	1209 s
878 m	1163 s
744 w	1003 m
600 m	883 w
490 w	662 vw
	575 vw

Optical microscopic observations

The TATB used as starting material for these studies was finely divided. The crystallites were too small to examine for morphological features at 625 ×. They were badly fractured, yellow, transparent and birefringent. At this magnification, all of the residues, whether from confined or unconfined decompositions, seemed to be sintered masses of extremely small crystallites, with less transparency and much less birefringence than the starting TATB. The number of phases present in any of the residues could not be ascertained.

The condensates from lower temperature unconfined decompositions appeared to have two phases. The condensate generated at 578 K for 340 min consisted of both very tiny, yellow, transparent, birefringent crystals and long, well formed, prismatic needles, that were birefringent perpendicular to the axis of the needle. Figure 7(a) is a photomicrograph of this sample. The two types of material were estimated to be present in nearly equal amounts. The condensate generated at 630 K appeared to be single phase, with very tiny, well formed, yellow, transparent, birefringent crystals. Figure 7(b) is a photomicrograph of this sample.

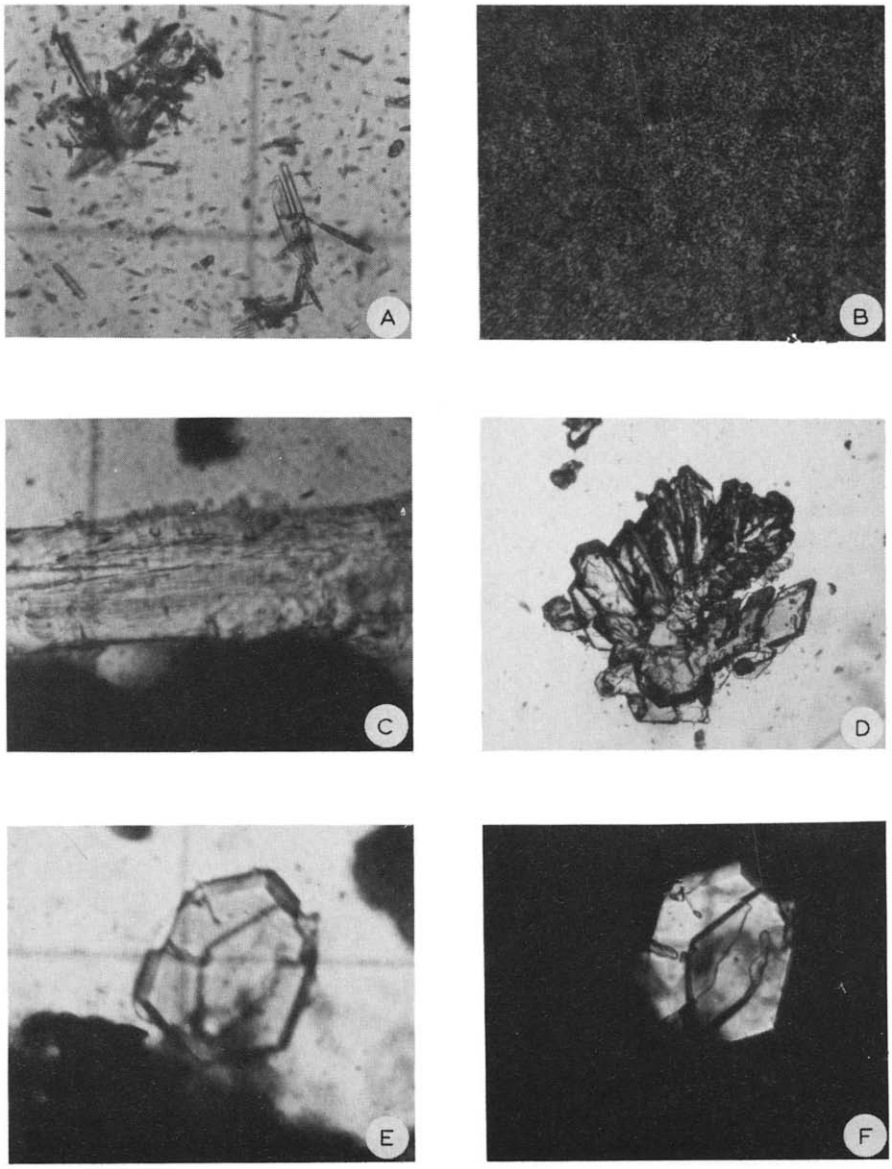

Fig. 7. Photo-micrographs of solid state decomposition products. (a) Condensate generated from an unconfined TATB decomposition at 578 K for 340 min, 325×; (b) condensate generated from an unconfined TATB decomposition at 630 K, 315×; (c) prismatic needle crystal, product found from the ODTX experiment at 597 K and 2.69 min, 315×, opaque second phase; (d) dendritic crystals, product found from the ODTX experiment, 125×; (e) hexagonal prismatic crystals, product from the ODTX experiment, opaque second phase, 315×; (f) as (e), but under polarized light illumination, 315×.

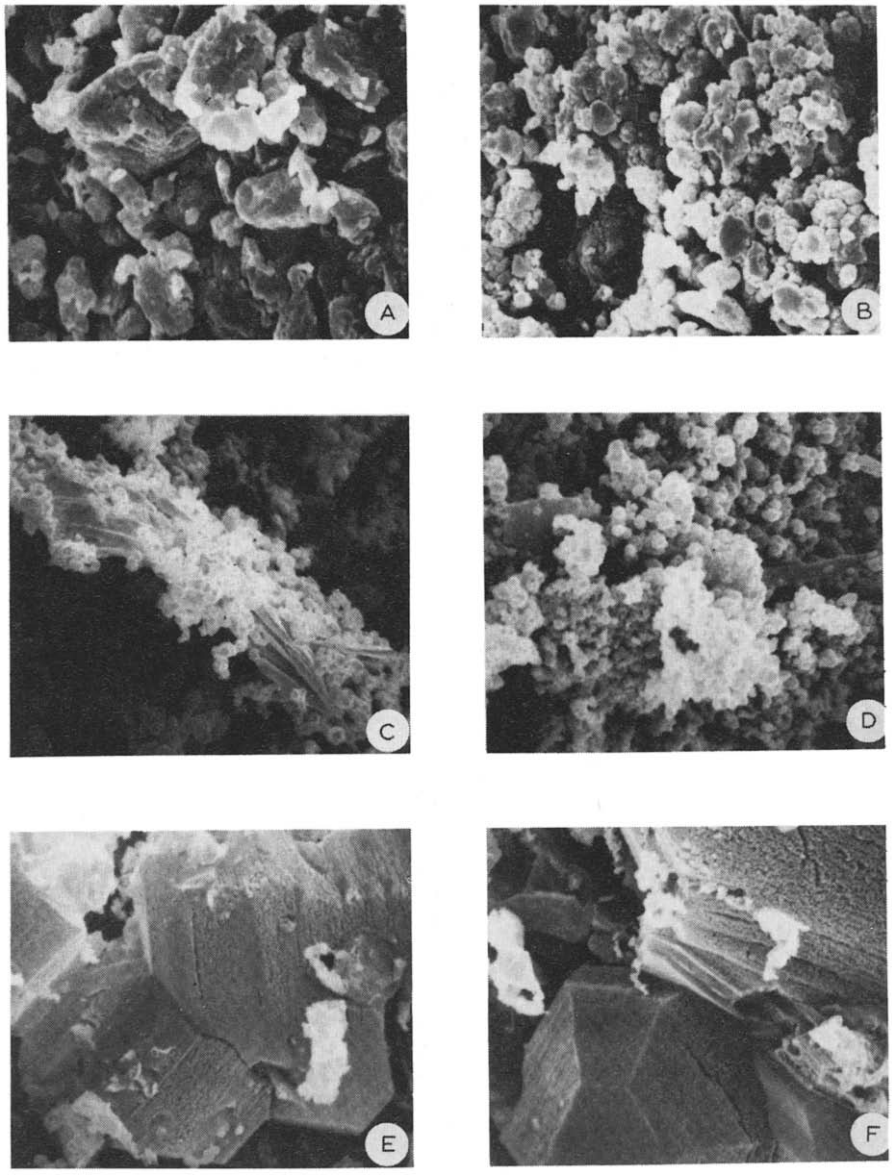

Fig. 8. SEM photos of TATB-B602 and of solid state decomposition products. All magnifications 3500×. (a) TATB-B602 starting materials; (b) condensate generated from a 578 K unconfined decomposition; (c) condensate generated from a 620 K unconfined decomposition; (d) condensate generated from a 630 K unconfined decomposition; (e) residue generated from a 620 K unconfined decomposition; (f) residue generated from a 630 K unconfined decomposition.

The products recovered from the ODTX experiment at $T = 597$ K, $t = 2.69$ min appeared to consist of at least two phases. The major phase was amorphous and opaque but the minor phase was crystalline. Three types of crystal were found.

(1) Long transparent needles which were birefringent perpendicular to the needle axis accounted for about 10% of the crystalline material present.

(2) Dendritic, yellow, transparent crystals, characteristic of vapor-phase growth accounted for about 45% of the crystalline material present.

(3) Well-formed hexagonal prisms that were transparent, yellow, and birefringent along the axes accounted for about 45% of the crystalline material present and appeared to have grown out of the opaque phase.

The similar morphology of the dendritic crystals and the prismatic crystals, suggests that these materials are the same phase. The number of needle crystals was very small. We did not ascertain whether they are the same phase as the other two crystalline forms. Figures 7(c)–(f) are photomicrographs of these samples.

SEM observations

Particle-size distributions and some of the morphological features of crystallites of TATB depend on details of the synthesis and whether the material had been sieved. A typical SEM picture of the TATB starting material is shown in Fig. 8(a). The TATB consists of very small crystallites with a broad distribution of particle sizes. The crystallites are poorly formed with many cracks and pits, but have no obvious porosity.

A characteristic SEM image of the condensate collected from a decomposition at 573 K is shown in Fig. 8(b). It appears to be very similar to the reference TATB. The condensate collected from a decomposition at 620 K is shown in Fig. 8(c). Two distinct phases are evident, one phase consisting of long, well-formed needles and the other with very small crystallites of hexagonal symmetry and an almost uniform size. The two phases are present in about equal amounts. An SEM of the condensate collected from a decomposition at 630 K is shown in Fig. 8(d). Three phases may be present. The preponderant phase has very small uniform crystallites with hexagonal symmetry, identical in size and morphology with those in Fig. 8(c). Also seen in this photo is a long needle-shaped crystallite and a large flat hexagonal plate.

The residues collected from unconfined decompositions at 620 and 630 K, respectively, are shown in Figs. 8(e) and 8(f). These consist of very large crystals of pseudo-hexagonal laminar plates. We have not shown a sample of a residue collected from a decomposition at 573 K whose particles are considerably larger than those of the original TATB, but much smaller than those in Figs. 8(e) and (f) and having different morphological features.

The material recovered from the ODTX experiment is shown in Fig. 9(a). This sample was hand picked and consisted of well-formed, transparent, yellow crystallites. We have not shown a sampling of the opaque material recovered in this experiment. These were rather large laminar chunks.

Finally, Fig. 9(b) is a SEM of a sample chunk of material recovered from

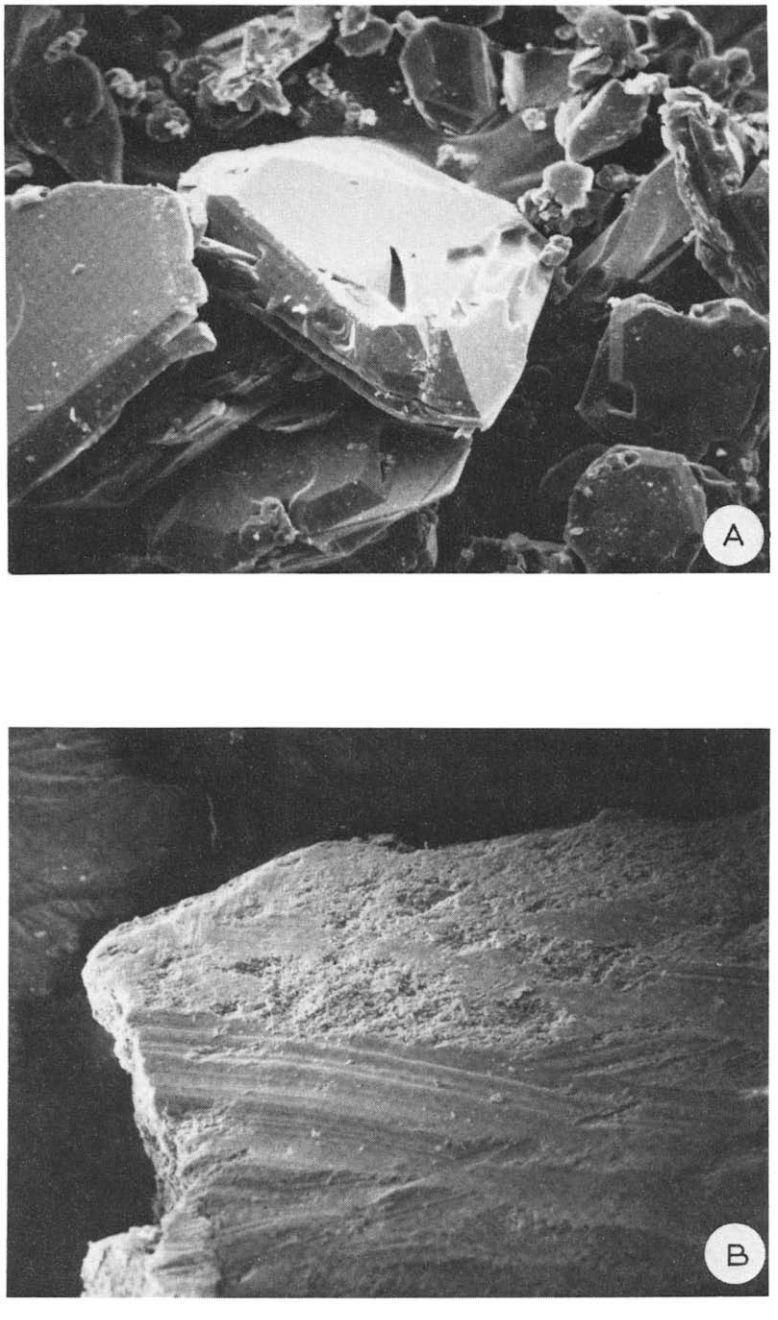

Fig. 9. SEM photos of confined TATB solid state decomposition products. (a) Crystals from ODTX experiment, 490×; (b) "crystalline" phase found in residues of a confined decomposition, 140×.

the residue of a confined decomposition at 529 K for 78 min. There appear to be two phases in this sample, a well crystallized portion (in this case a twinned crystal) and a very porous phase.

DISCUSSION

The experimental observations complement the information derived from enthalpic data from unconfined decompositions and the gaseous product evolution data from confined decompositions.

The spectral and microscopic data imply that almost no decomposition had occurred in the residues obtained from confined decompositions, since the spectral features of the residues were identical with those of the starting TATB. This conclusion is also consistent with the gas evolution data [8]. The only observations, in this work, that are not fully consistent with such a conclusion are the SEM data for an apparent crystalline phase, Fig. 9(b), that suggests the presence of a second product, and the fact that small changes are seen in the spectral data, Fig. 2.

The spectral differences between TATB and the products collected from the ODTX experiment are minor (Fig. 2). However, the microscopic and SEM data do indicate three apparent phases. This information can be interpreted in (at least) two ways. First, the three phases may really be TATB in two morphological configurations (separate or mixed) that are virtually identical in structure. (The two transparent configurations are separate morphological entities; the opaque is a mixture of the two.) Second, there are two or more phases, but one phase is predominant, and that phase is very slightly decomposed TATB. These products are those collected on the ODTX anvils. They were present within the decomposing sample at $t = t_x$ and are low vapor pressure species. Furthermore, the remains of the main charge of TATB was a charred mass. X-Ray powder patterns of the collected transparent crystals, kindly provided by Cady [12], indicated that the structure of these materials was very similar to, but not identical with that of TATB. We are at present unable to choose between the suggested interpretations.

A question remains as to whether TATB exists as a number of polymorphs, or whether there may be one or more intermediates that are very similar in structure to TATB. In a recent paper, Kolb and Rizzo [13] have reported two new crystalline forms of TATB. The crystal chemistry of TATB remains challengingly unsettled at this time.

The spectral, microscopic and SEM data acquired on the condensates collected from unconfined decompositions are consistent with there being a number of different solid state products. The presence of some TATB is expected since it volatilizes congruently [4,14]. If we assume the presence of TATB, we can try to deconvolute the spectral data shown in Figs. 3 and 4

and listed in Table 1. We first subtract out TATB spectral features from the individual condensate spectra. Then we subtract out the remaining spectral features of the condensate formed at the lower temperature from that of the condensate formed at the next higher temperature. This procedure is tantamount to assuming a reaction sequence (for the condensates only) of

TABLE 3

Condensate spectra decomposition (wavenumbers)
Assumptions: TATB → A → B → C
At 573 K condensate is TATB + A; at 619 K condensate is TATB + A + B; at 629 K condensate is TATB + A + B + C.

A	B	C
3615 w	3430 m	3356 w
3410 w	3379 m	1316 w
3302 vs	3239 vs	1260 s
3145 vw	2960 s	1095 s
3063 vw	2924 vs	619 w
2785 vw	2852 s	479 w
2700 vw	1573 m	420 m
2645 vs	1507 vw	
2590 vw	1585 s	
2500 w	1316 w	
2375 w	1120 vvw	
1657 s	1084 vvw	
1583 s	619 w	
1558 s	471 w	
1463 s		
1344 s		
1283 vs		
1128 vw		
1090 m		
1074 w		
995 s		
978 vw		
922 vw		
904 vw		
889 s		
868 w		
853 w		
820 m		
683 w		
619 w		
594 w		
487 w		

the type

$$\begin{aligned} &\text{TATB} \rightarrow \text{A} && T = 573\ \text{K} \\ &\text{TATB} \rightarrow \text{A} + \text{B} && T = 619\ \text{K} \\ &\text{TATB} \rightarrow \text{A} + \text{B} + \text{C} && T = 624\ \text{K} \end{aligned}$$

The results are listed in Table 3. The columns labelled A, B and C are the spectral features of the A, B and C, respectively, which may actually be mixtures of product species. Products A and B probably still contain N–H bonds, N–O bonds, and some intact benzene rings, by analogy with observed band frequencies and intensities. (See, for example, ref. [15].) The spectra indicate that product C is almost devoid of N–H bonds.

The spectra of the residues from unconfined TATB decompositions (Figs. 5 and 6 and Table 2) show broad and complex bands. However, there are no remaining features clearly attributable to TATB. It appears as if the spectral features of the residue collected at the higher decomposition temperature are similar to those for the residues collected at the lower temperature, but with some additional bands. Furthermore, the spectra of these residues do not correspond with those of products A, B or C in Table 3. The SEM data seem to show a gradual growth of crystallites with increasing decomposition temperature. We speculate that the composition change is gradual, based on the spectra and SEM pictures of the residues.

By using the gaseous product production [9], the vaporization observations in TATB [4,14], the spectral, microscopic and SEM data on condensates and residues generated during unconfined TATB decompositions, we can model the reaction as

$$\text{TATB} \xrightarrow{\Delta} \text{TATB}_{(c)} + \sum_i \text{A}^i_{(c)} + \sum_j \text{A}^j_{(g)} + \sum_p \text{D}^p_{(s)} \text{ at } T_1$$

$$\text{TATB} \xrightarrow{\Delta} \text{TATB}_{(c)} + \sum_i \text{A}^i_{(c)} + \sum_j \text{A}^j_{(g)} + \sum_i \text{B}^i_{(c)} + \sum_j \text{B}^j_{(g)} + \sum_q \text{D}^q_{(s)} \text{ at } T_2$$

$$\text{TATB} \xrightarrow{\Delta} \text{TATB}_{(c)} + \sum_i \text{A}^i_{(c)} + \sum_j \text{A}^j_{(g)} + \sum_i \text{B}^i_{(c)} + \sum_j \text{B}^j_{(g)} + \sum_i \text{C}^i_{(c)} + \sum_j \text{C}^j_{(g)} + \sum_r \text{D}^r_{(s)} \text{ at } T_3$$

where $T_3 > T_2 > T_1$. Here the subscripts (c), (g) and (s) refer to the state of the products, i.e. volatile solids (condensates), gaseous products and nonvolatile solids, respectively. The superscripts denote product species. This model describes the reaction as consisting of a series of consecutive steps along with concurrent reaction for the unconfined decomposition, in contrast to the conclusions drawn on the basis of the enthalpic changes in which the reaction was interpreted as a series of consecutive reactions [9]. The two interpretations could be consistent if the enthalpic changes associated with the production of products $\text{D}_{(s)}$ are small compared to all other heat effects.

Several inconsistencies regarding the thermal decomposition of TATB remain; three of these are mentioned. (1) Why did Farber and Srivastava [2] in their mass spectroscopic study find TATB decomposing at temperatures where Garza [4] and Kolb and Garza [14] found congruent vaporization? (2) Does the decomposition mechanism depend upon whether or not the TATB is confined? Our previous reports [8,9] and this work tend to imply that it does, since the rate laws are different and the initial stage of the confined reaction is endothermic while the unconfined reactions are exothermic. Examination of the solid state products for the confined decomposition show so little decomposition that nothing can be inferred with regard to this question. Also, the temperatures for the isothermal reactions were much higher for the unconfined decomposition than for the confined ones. (3) Is water abstraction important in the decomposition as reported by Andrews et al. [3]? We think not, on the basis of the gaseous evolution data [8]. If water abstraction took place, the product expected is a furozan [16]. There are no

spectral features among any of the solid state products that are expected for a furozan, but there is not enough evidence for a positive conclusion.

CONCLUSIONS

Spectral, microscopic and SEM examination of the solid state products formed by the decomposition of confined TATB show that virtually no decomposition takes place at temperatures as high as 630 K and times up to t_x. Examination of those solid state products formed by the decomposition of unconfined TATB show that TATB and several other phases are present in the condensates and residues.

ACKNOWLEDGEMENTS

We wish to thank Drs. Howard W. Cady, Tomas B. Hirschfeld, John R. Kolb, Herman R. Leider, and Messrs. Raul Garza and James W. Fischer for their discussions. We wish to particularly thank Mrs. Patricia C. Crawford for her help.

REFERENCES

1 H.W. Cady and A.C. Larson, Acta Crystallogr. 18 (1965) 485.
2 M. Farber and R.D. Srivastava, A Mass-Spectrometric Investigation of the Decomposi-

tion Products of Advanced Propellants and Explosives, Space Sciences, Monrovia, CA, 1979.
3 G.H. Andrews, R.N. Rogers and G.W. Taylor, Proc. 5th Annual ERDA Compatibility Meeting, Mound Laboratory, Oct. 1977.
4 R.G. Garza, Lawrence Livermore National Laboratory Report UCRL 82723, 1979.
5 J.L. Janney and R.N. Rogers, Experimental Thermochemical Observations of Condensed Phase Reactions, Proc. North American Thermal Analysis Society, New Orleans, LA, 1981.
6 E. Catalano, R. McGuire, E. Lee, E. Wrenn, D. Ornellas and J. Walton, 6th Symposium on Detonation, Naval Weapons Center, White Oak, MD. Aug. 24–27, 1976.
7 R.N. Rogers, Thermochim. Acta, 11 (1975) 131.
8 E. Catalano and C.E. Rolon, Thermochim. Acta, 61 (1983) 37.
9 E. Catalano and P.C. Crawford, Thermochim. Acta, 61 (1983) 23.
10 B.L. Deopura and V.D. Gupta, J. Chem. Phys., 54 (1971) 4013.
11 T.G. Towns, Lawrence Livermore National Laboratory Report UCRL 85914, 1981.
12 H. Cady, private communication, 1981.
13 J.R. Kolb and H.F. Rizzo, Propellants Explosives 4 (1979) 10.
14 J.R. Kolb and R.G. Garza, Lawrence Livermore National Laboratory Report UCRL 85971, 1981.
15 K. Nakaniski, Infrared Absorption Spectroscopy, Holden-Day, San Francisco, CA, 1962.
16 R. McGuire, private communication, 1981.

DISCLAIMER